

# WASP-10b: a $3M_J$ , gas-giant planet transiting a late-type K star

D.J. Christian<sup>1,17\*</sup>, N.P. Gibson<sup>1</sup>, E.K. Simpson<sup>1</sup>, R.A. Street<sup>1,2</sup>, I. Skillen<sup>3</sup>,  
 D. Pollacco<sup>1</sup>, A. Collier Cameron<sup>4</sup>, Y.C. Joshi<sup>1</sup>, F.P. Keenan<sup>1</sup>, H.C. Stempels<sup>4</sup>,  
 C.A. Haswell<sup>5</sup>, K. Horne<sup>4</sup>, D.R. Anderson<sup>5</sup>, S. Bentley<sup>6</sup>, F. Bouchy<sup>7,8</sup>, W.I. Clarkson<sup>5,16</sup>,  
 B. Enoch<sup>5</sup>, L. Hebb<sup>4</sup>, G. Hébrard<sup>7</sup>, C. Hellier<sup>6</sup>, J. Irwin<sup>9</sup>, S.R. Kane<sup>10</sup>,  
 T.A. Lister<sup>2,4,6</sup>, B. Loeillet<sup>11</sup>, P. Maxted<sup>6</sup>, M. Mayor<sup>12</sup>, I. McDonald<sup>6</sup>, C. Moutou<sup>11</sup>,  
 A.J. Norton<sup>5</sup>, N. Parley<sup>5</sup>, F. Pont<sup>12,13</sup>, D. Queloz<sup>12</sup>, R. Ryans<sup>1</sup>, B. Smalley<sup>6</sup>,  
 A.M.S. Smith<sup>4</sup>, I. Todd<sup>1</sup>, S. Udry<sup>12</sup>, R.G. West<sup>14</sup>, P.J. Wheatley<sup>15</sup>, D.M. Wilson<sup>6</sup>

<sup>1</sup> *Astrophysics Research Centre, School of Mathematics & Physics, Queen's University, University Road, Belfast, BT7 1NN, UK*

<sup>2</sup> *Las Cumbres Observatory, 6740 Cortona Dr. Suite 102, Santa Barbara, CA 93117, USA*

<sup>3</sup> *Isaac Newton Group of Telescopes, Apartado de Correos 321, E-38700 Santa Cruz de la Palma, Tenerife, Spain*

<sup>4</sup> *School of Physics and Astronomy, University of St Andrews, North Haugh, St Andrews, Fife KY16 9SS, UK*

<sup>5</sup> *Department of Physics and Astronomy, The Open University, Milton Keynes, MK7 6AA, UK*

<sup>6</sup> *Astrophysics Group, Keele University, Staffordshire, ST5 5BG*

<sup>7</sup> *Institut d'Astrophysique de Paris, CNRS (UMR 7095) – Université Pierre & Marie Curie, 98<sup>bis</sup> bvd. Arago, 75014 Paris, France*

<sup>8</sup> *Observatoire de Haute-Provence, 04870 St Michel l'Observatoire, France*

<sup>9</sup> *Harvard/Smithsonian Center for Astrophysics, 60 Garden Street, Cambridge, MA 02138, USA*

<sup>10</sup> *Michelson Science Center, Caltech, MS 100-22, 770 South Wilson Avenue Pasadena, CA 91125, USA*

<sup>11</sup> *Laboratoire d'Astrophysique de Marseille, BP 8, 13376 Marseille Cedex 12, France*

<sup>12</sup> *Observatoire de Genève, Université de Genève, 51 Ch. des Maillettes, 1290 Sauverny, Switzerland*

<sup>13</sup> *School of Physics, University of Exeter, Stocker Road, Exeter EX4 4QL*

<sup>14</sup> *Department of Physics and Astronomy, University of Leicester, Leicester, LE1 7RH, UK*

<sup>15</sup> *Department of Physics, University of Warwick, Coventry CV4 7AL, UK*

<sup>16</sup> *STScI, 3700 San Martin Drive, Baltimore, MD 21218, USA*

<sup>17</sup> *Department of Physics and Astronomy, California State University Northridge, 18111 Nordhoff Street, Northridge, CA 91330-8268, USA*

Accepted 2008 October ??; Received 2008 September ??; in original form 2008 May ??

## ABSTRACT

We report the discovery of WASP-10b, a new transiting extrasolar planet (ESP) discovered by the WASP Consortium and confirmed using NOT FIES and SOPHIE radial velocity data. A 3.09 day period, 29 mmag transit depth, and 2.36 hour duration are derived for WASP-10b using WASP and high precision photometric observations. Simultaneous fitting to the photometric and radial velocity data using a Markov-chain Monte Carlo procedure leads to a planet radius of  $1.28R_J$ , a mass of  $2.96M_J$  and eccentricity of  $\approx 0.06$ . WASP-10b is one of the more massive transiting ESPs, and we compare its characteristics to the current sample of transiting ESP, where there is currently little information for masses greater than  $\approx 2M_J$  and non-zero eccentricities. WASP-10's host star, GSC 2752-00114 (USNO-B1.0 1214-0586164) is among the fainter stars in the WASP sample, with  $V=12.7$  and a spectral type of K5. This result shows promise for future late-type dwarf star surveys.

**Key words:** methods: data analysis – stars: planetary systems – techniques: radial velocities – techniques: photometric

## 1 INTRODUCTION

Photometric transit observations of extrasolar planets (ESP) are important because the transit strongly constrains their

\* E-mail: d.christian@qub.ac.uk

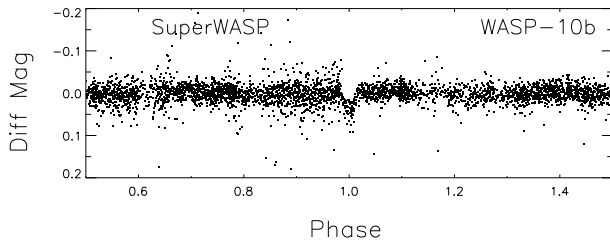


**Figure 1.** (a.) The *top* panel shows the SuperWASP light curve for WASP-10b (1SWASP J231558.30+312746.4). All the data (apart from that from SuperWASP-N) were averaged in 300 second bins. The data were phased using the ephemeris,  $T_O = 2454357.85808^{+0.00041}_{-0.00036}$   $P = 3.09276$  days.

orbital inclination and allows accurate physical parameters for the planet to be derived. Their mass-radius relation allows us to probe their internal structure and is vital to our understanding of orbital migration and planetary formation. The radial velocity measurements which are used to confirm a candidate transiting ESP also provide more complete information on the orbital eccentricity.

As wide field photometric transit surveys have collected additional sky and temporal coverage, and understood their noise components (Collier Cameron et al. 2007a; Smith et al. 2007), the number of transiting ESP has grown to over 50 in line with earlier predictions (Horne 2003). Recently one such survey, SuperWASP (Pollacco et al. 2006) published its first 5 confirmed ESP, all of which have periods of less than 3 days (Anderson et al. 2008; Collier Cameron et al. 2007b; Pollacco et al. 2008; Wilson et al. 2008), and reported an additional  $10^1$  (Hellier et al. 2008; Hebb et al. 2008; Joshi et al. 2008; West et al. 2008). SuperWASP is performing a "shallow-but-wide" transit search, designed to find planets that are not only sufficiently bright ( $9 < V < 13$ ) for high-precision radial velocity follow-up to be feasible on telescopes of moderate aperture, but also for detailed studies such as transmission spectroscopy during transits. Details of the WASP project and observatory infrastructure are described in Pollacco et al. (2006).

In this paper we present the WASP photometry of 1SWASP J231558.30+312746.4 (GSC 2752-00114), higher precision photometric follow-up observations with the MERCATOR and Tenagra telescopes, and high precision radial velocity observations with the Nordic Optical Telescope new Fibre-fed Echelle Spectrograph (FIES) and the OHP SOPHIE collaboration. These observations lead to the discovery and confirmation of a new, relatively high mass, gas-giant exoplanet, WASP-10b.

## 2 OBSERVATIONS

1SWASP J231558.30+312746.4 (GSC 2752-00114) was monitored by SuperWASP-N starting in 2004. SuperWASP is a multi-camera telescope system with SuperWASP-North located in La Palma and consisting of 8 Canon 200-mm f/1.8 lenses each coupled to e2v 2048 x 2048 pixel back illuminated CCDs. This combination of lens and camera yields a

field of view of  $7.8^\circ \times 7.8^\circ$  with an angular size of  $14.2''$  per pixel. During 2004, SuperWASP was run with 4 or 5 cameras as the operations moved from commissioning to routine automated observing. We show the WASP-10b SuperWASP light curve in Figure 1.

### 2.1 Higher Precision Photometry

We obtained photometry of WASP-10 with the MEROPE instrument on the 1.2m MERCATOR Telescope in V-band on 1 September 2007. Only a partial transit was observed due to uncertainties in the period and epoch from the SuperWASP data. Observations were in the V-band with  $2 \times 2$  binning over  $\sim 2.9$  hours. Despite clear conditions, exposure times were varied from 25-30s to account for changes in seeing and to keep below the saturation limits of the chip. This allowed 170 images to be taken. There was a drift of only 1 binned pixel in x and y on the chip during the run. The MEROPE images were first de-biased and flat fielded with combined twilight flats using IRAF and the apphot package to obtain aperture photometry of the target and 5 nearby companion stars using a 10 pixel radius. Finally, the light curve was extracted and normalized to reveal a depth of  $\sim 33$  mmag.

Further observations of WASP-10 were taken as part of an observing program sponsored by the Las Cumbres Observatory Global Telescope Network<sup>2</sup> on the Tenagra II, 0.81m F7 Ritchey-Chretien telescope sited in the Sonora desert in S. Arizona, USA. The science camera contains a  $1k \times 1k$  SITe CCD with a pixel scale of 0.87 arcsec/pixel and a field of view of  $14.8' \times 14.8'$ . The filter set is the standard Johnson/Cousins/Bessel UBVR set and the data presented here have been taken in I band.

Calibration frames were obtained automatically every twilight, and the data were de-biased and flat-fielded using the calibration section of the SuperWASP pipeline. Object detection and aperture photometry was then performed using daophot (Stetson 2007) within IRAF. Differential photometry was derived from a selection of typically 5 to 10 comparison stars within the frame.

These confirmed the object had a sharp egress with an amplitude of  $0.033 \pm 0.001$ mag. The MERCATOR V and Tenagra I light curves show consistent transit depths, confirming that the companion is a transiting ESP.

### 2.2 Spectroscopic Follow-up

We obtained high precision radial velocity (RV) follow-up observations of WASP-10 with the 2.5m Nordic Optical Telescope (NOT) new Fibre-fed Echelle Spectrograph (FIES), supplemented with observations from the Observatoire de Haute-Provence's 1.93 m telescope and the SOPHIE spectrograph (Bouchy et al. 2006). We present a summary of the FIES and SOPHIE RV data in Table 1.

#### 2.2.1 NOT and FIES

Spectroscopic observations were obtained using the new FIES spectrograph mounted on the NOT Telescope. A to-

<sup>1</sup> <http://www.inscience.ch/transits/>

<sup>2</sup> [www.lcogt.net](http://www.lcogt.net)

**Table 1.** Journal of radial-velocity measurements for WASP-10 (1SWASP J231558.30+312746.4, USNO-B1.0 1214-0586164). Stellar coordinates are for the photometric apertures; the USNO-B1.0 number denotes the star for which the radial-velocity measurements were secured. The quoted uncertainties in the radial velocity errors include components due to photon noise (Section 2.2) and  $10 \text{ m s}^{-1}$  of jitter (Section 3.2) added in quadrature.

BJD	$t_{\text{exp}}$ (s)	$V_r$ $\text{km s}^{-1}$
<i>FIES</i>		
2454437.540	2400	$-11.028 \pm 0.026$
2454463.377	2400	$-11.941 \pm 0.030$
2454465.342	2400	$-11.003 \pm 0.018$
2454466.335	2400	$-11.804 \pm 0.021$
2454490.329	2400	$-11.013 \pm 0.143$
2454490.358	2400	$-10.990 \pm 0.120$
2454491.340	2400	$-11.955 \pm 0.024$
<i>SOPHIE</i>		
2454340.569	3300	$-11.657 \pm 0.008$
2454342.505	3600	$-11.575 \pm 0.011$
2454508.262	1680	$-11.027 \pm 0.014$
2454509.268	1680	$-11.336 \pm 0.017$
2454510.276	1680	$-11.990 \pm 0.020$
2454511.262	1680	$-11.135 \pm 0.016$
2454512.262	1680	$-11.244 \pm 0.016$

tal of seven radial velocity points were obtained during 2 December 2007, 28–31 December 2007 and 24–25 January 2008. WASP-10 required observations with an exposure time of 2400s due its relative faintness ( $V=12.7$ ) yielding a peak signal-to-noise ratio per resolution element of  $\approx 60$ –70 in the  $H\alpha$  region. FIES was used in medium resolution mode with  $R=46000$  with simultaneous ThAr calibration. We used the bespoke data reduction package FIEStool<sup>3</sup> to extract the spectra and a specially developed IDL line-fitting code to obtain radial velocities with a precision of  $15$ – $25 \text{ m s}^{-1}$  (except for the poor night of 24 January 2008, JD 2454490).

### 2.2.2 OHP 1.9m and SOPHIE

Additional radial velocity measurements were taken for WASP-10 on 2007 August 29 and 30, and again between 2008 Feb 11 and 15 with the OHP 1.93 m telescope and the SOPHIE spectrograph (Bouchy et al. 2006), a total of 7 usable spectra were acquired. We used SOPHIE in its high efficiency mode, acquiring simultaneous star and sky spectra through separate fibers with a resolution of  $R=40000$ . Thorium-Argon calibration images were taken at the start and end of each night, and at 2- to 3-hourly intervals throughout the night. The radial-velocity drift never exceeded  $2$ – $3 \text{ m s}^{-1}$ , even on a night-to-night basis. Although errors for each radial velocity measurement are limited by the photon-noise. Thus, the average radial velocity error is  $\approx 14 \text{ m s}^{-1}$  and includes the  $2$ – $3 \text{ m s}^{-1}$  systematic error and the contribution from the photon-noise. Typical signal-to-noise ratio estimates for each spectra were  $\approx 30$  (near  $5500 \text{ \AA}$ ). The SOPHIE WASP-10 spectra were cross-correlated against a K5V template provided by the SOPHIE control

**Table 2.** Stellar parameters for WASP-10. The last 5 parameters were derived from the SME analysis of the FIES spectroscopy.

Parameter	WASP-10
RA (J2000)	23 15 58.3
Dec (J2000)	+31 27 46.4
$V$	12.7
distance	$90 \pm 20 \text{ pc}$
$T_{\text{eff}}$	$4675 \pm 100 \text{ K}$
$\log g$	$4.40 \pm 0.20$
[M/H]	$0.03 \pm 0.20$
$v \sin i$	$< 6 \text{ km s}^{-1}$
$v_{\text{rad}}$	$-11.44 \pm 0.03 \text{ km s}^{-1}$

and reduction software. Typical FWHM and contrasts for these spectra were  $\approx 10.2$ – $10.4 \text{ km s}^{-1}$  and  $30$ – $31\%$ , respectively. The cross-correlation techniques and derivation of errors in the radial velocity measurements are presented in Pollacco et al. (2008).

## 3 RESULTS AND ANALYSIS

### 3.1 Stellar parameters

We merged all available WASP-10 FIES spectra into one high-quality spectrum in order to perform a detailed spectroscopic analysis of the stellar atmospheric properties. Radial velocity signatures were carefully removed during the process. This merged spectrum was then continuum-normalized with a low order polynomial to retain the shape of the broadest spectral features. The total signal-to-noise ratio of the combined spectrum was  $\approx 180$  per pixel. We were not able to include the SOPHIE spectra in this analysis, because these spectra were obtained in the HE (high-efficiency) mode, which is known to suffer from problems with removal of the blaze function.

As previously undertaken for our analysis of WASP-1 (Stempels et al. 2007), and WASP-3 (Pollacco et al. 2008) we employed the methodology of Valenti & Fischer (2005), using the same tools, techniques and model atmosphere grid. We used the package *Spectroscopy Made Easy* (SME) (Valenti & Piskunov 1996), which combines spectral synthesis with multidimensional  $\chi^2$  minimization to determine which atmospheric parameters best reproduce the observed spectrum of WASP-10 (effective temperature  $T_{\text{eff}}$ , surface gravity  $\log g$ , metallicity [M/H], projected radial velocity  $v \sin i$ , systemic radial velocity  $v_{\text{rad}}$ , microturbulence  $v_{\text{mic}}$  and the macroturbulence  $v_{\text{mac}}$ ).

The four spectral regions we used in our analysis are: (1)  $5160$ – $5190 \text{ \AA}$ , covering the gravity-sensitive Mg b triplet (2)  $5850$ – $5950 \text{ \AA}$ , with the temperature and gravity-sensitive Na I D doublet; (3)  $6000$ – $6210 \text{ \AA}$ , containing a wealth of different metal lines, providing leverage on the metallicity, and (4)  $6520$ – $6600 \text{ \AA}$ , covering the strongly temperature-sensitive H-alpha line. In addition we analyzed a small region around the Li I 6708 line to possibly derive a lithium abundance, but no Li I 6708 was detected for WASP-10. The parameters we obtained from this analysis are listed in Table 2. In addi-

<sup>3</sup> <http://www.not.iac.es/instruments/fies/fiestool/FIEStool.html>

tion to the spectral analysis, we also use available photometry (from NOMAD, TASS4 and CMC14 catalogues), plus 2MASS to estimate the effective temperature using the Infrared Flux Method (Blackwell & Shallis 1977). This yields  $T_{\text{eff}} = 4650 \pm 120$  K, which is in agreement with the spectroscopic analysis and a spectral type of K5. The characteristics of WASP-10 are also given in Table 2.

### 3.2 Markov-chain Monte Carlo analysis

Transit timing and the radial-velocity measurements provide detailed information about the orbit. We modelled WASP-10b's transit photometry and the reflex motion of the host star simultaneously using the Markov-chain Monte-Carlo algorithm described in detail by Collier Cameron et al. (2007a), and the same techniques that were applied to WASP-3 by Pollacco et al. (2008) to which we refer the reader for more details.

We find WASP-10b to have a radius  $1.28^{+0.08}_{-0.09} R_J$ , mass of  $2.96^{+0.22}_{-0.17} M_J$  and a significant non-zero eccentricity of  $0.059^{+0.014}_{-0.004}$ . The best fit solution for the MCMC model for a circular orbit ( $e = 0$ ) has a  $\chi^2$  55 higher than the solution with non-zero eccentricity, and thus, the eccentricity is significant at  $> 99.6\%$  confidence level using the  $F$  test. The values of the parameters of the optimal solution are given, together with their associated  $1\text{-}\sigma$  confidence intervals, in Table 3. The FIES+SOPHIE radial-velocity data measurements are plotted in Figure 2 together with the best-fitting global fit to the SuperWASP-N, MERCATOR, and Tenagra transit photometry.

### 3.3 Line-bisector variation

Line bisectors have been shown to be a powerful diagnostic in distinguishing true extra-solar planets from blended and eclipsing stellar systems chromospheric activity (Queloz et al. 2001). Torres et al. (2004) showed, that for OGLE-TR-33 line asymmetries which changed with a 1.95 day period, it was a blended system. From the cross-correlation function (CCF) we obtained the line bisectors and these are plotted, as a function of RV, in Figure 3.

We quantified the significance of the bisector variation as follows. We determined the inverse-variance weighted averages of the RV and bisector span as

$$\hat{v} = \frac{\sum_i v_i w_i}{\sum_i w_i}; \quad \hat{b} = \frac{\sum_i b_i w_i}{\sum_i w_i}$$

where the  $v_i$  and  $b_i$  are the RV and span bisector values respectively and the weights  $w_i$  are the inverse variances of the individual bisector measurements. The uncertainty in the span bisector is assumed to be 2.5 times the uncertainty on the RV in our data. If we define  $x_i = v_i - \hat{v}$  and  $y_i = b_i - \hat{b}$ , then the slope is determined as

$$\hat{a} = \frac{\sum_i x_i y_i w_i}{\sum_i x_i^2 w_i}; \quad \text{Var}(\hat{a}) = \frac{1}{\sum_i x_i^2 w_i}$$

The value of the scaling factor  $\hat{a}$  is determined with signal-to-noise ratio

$$\text{SNR} = \frac{\hat{a}}{\sqrt{\text{Var}(\hat{a})}}$$

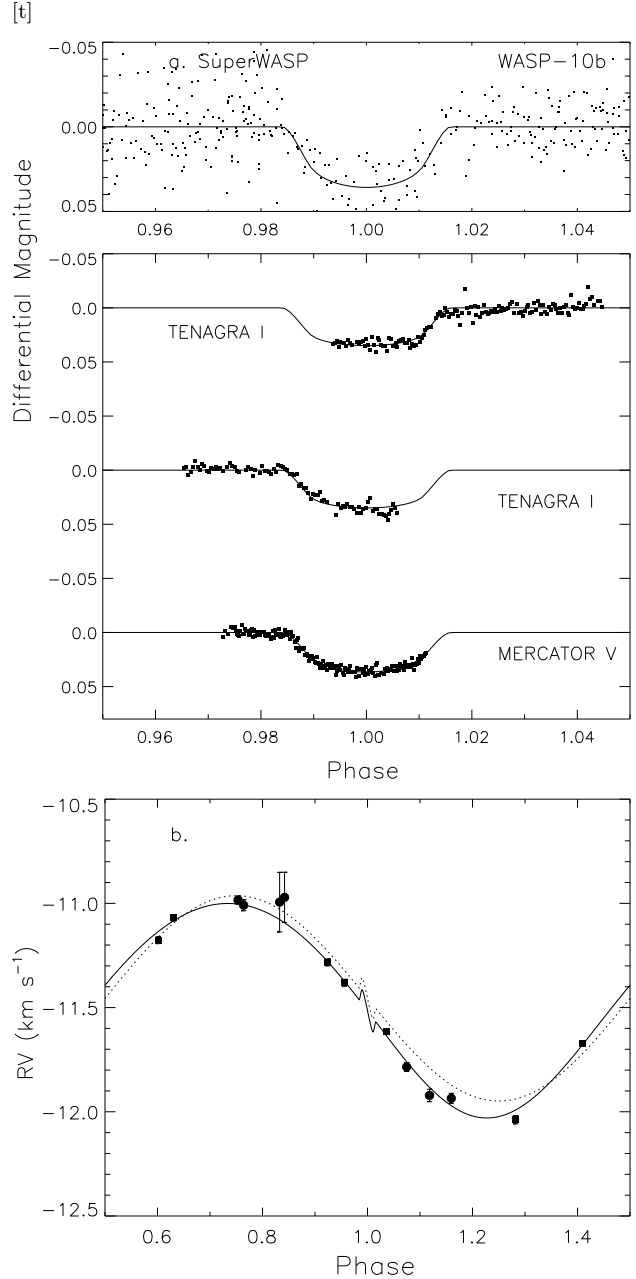


**Figure 2.** Simultaneous Markov-chain Monte Carlo (MCMC) solutions to the WASP-10 photometry and radial velocity data. a. *Top panels* show the MCMC solutions to the combined SuperWASP-N, MERCATOR V, and Tenagra I band photometry. b. The *lower panel* shows the MCMC solution to the FIES + SOPHIE radial velocity (RV) data. (FIES RVs are shown as filled circles and SOPHIE as filled squares). The model fit to the RV data includes orbital eccentricity (solid line), and for a circular orbit (dashed line). Both RV models also include the Rossiter-McLaughlin effect, which is small for this system given the low  $v \sin i$  of the host star ( $< 6 \text{ km s}^{-1}$ ).

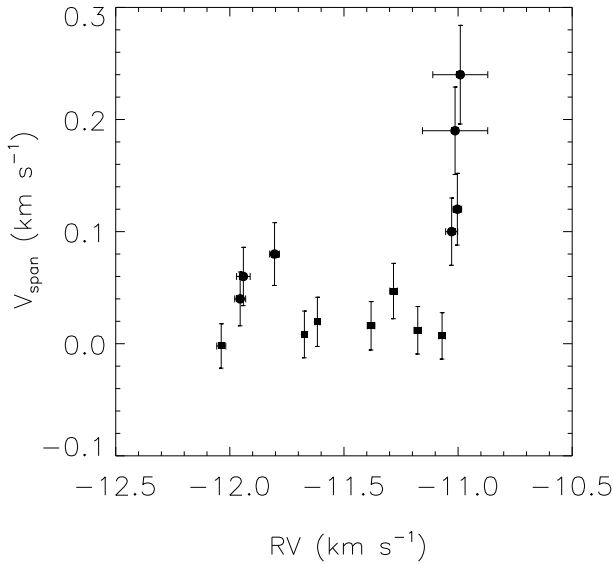


**Figure 3.** Line bisectors as a function of radial velocity (RV) for WASP-10. Plot symbols are the same as Figure 2. Analysis of these line-bisectors for WASP-10 does not show a correlation between the bisector velocity ( $V_{span}$ ) and stellar radial-velocity (see text).

We obtain  $\text{SNR} = 1.16$ , indicating a non-significant correlation between the bisector span and radial velocity variations. This demonstrates that the cross-correlation function remains symmetric, and that the radial-velocity variations are not likely to be caused by line-of-site binarity or stellar activity and indicate WASP-10b is an exoplanet.

## 4 DISCUSSION

Photometric surveys have now provided a large sample of transiting ESP that can be used to determine their mass-radius relation and provide constraints on their compositions. Here we presented the discovery of a new ESP with a mass of  $2.96M_J$ ,  $1.28R_J$  radius, and a significant eccentricity of  $0.059^{+0.014}_{-0.004}$ . We now discuss the properties of WASP-10b in relation to the current sample of transiting ESP, starting with its non-zero eccentricity.

Most of the current sample of published transiting ESP have orbits consistent with being circular and are fit with models using zero eccentricity as is expected for short-period planets in orbits with semi-major axes  $< 0.2$  AU. Recent work (Jackson et al. 2008; Mardling 2007 and references therein) has investigated the effects of tidal dissipation on the orbits of short period ESP. The evolution of the orbital eccentricity appears to be driven primarily by tidal dissipation within the planet, giving a circularisation timescale substantially less than 1 Gyr for typical tidal dissipation parameter,  $Q_p = 10^5$  to  $10^6$ . WASP-10 is a K dwarf with a spin period of 12 days and  $J-K=0.62$  and is rotating more slowly than stars of comparable colour in the Hyades (Terndrup et al. 2000). This suggests a rotational age between 600 Myr and 1 Gyr. Thus, the persistence of substantial orbital eccentricity in WASP-10b is therefore surprising.

**Table 3.** WASP-10 system parameters and  $1-\sigma$  error limits derived from MCMC analysis.

Parameter	Symbol	Value
Transit epoch (BJD)	$T_0$	$2454357.85808^{+0.00041}_{-0.00036}$ days
Orbital period	$P$	$3.0927636^{+0.0000094}_{-0.000021}$ days
Planet/star area ratio	$(R_p/R_s)^2$	$0.029^{+0.001}_{-0.001}$
Transit duration	$t_T$	$0.098181^{+0.0019}_{-0.0015}$ days
Impact parameter	$b$	$0.568^{+0.054}_{-0.084} R_*$
Stellar reflex velocity	$K_1$	$0.5201^{+0.0084}_{-0.010}$ km s $^{-1}$
Centre-of-mass velocity	$\gamma$	$-11.4854^{+0.0012}_{-0.0034}$ km s $^{-1}$
Orbital semimajor axis	$a$	$0.0369^{+0.0012}_{-0.0014}$ AU
Orbital inclination	$I$	$86.9^{+0.6}_{-0.5}$ degrees
Orb. eccentricity	$e$	$0.059^{+0.014}_{-0.004}$
Arg. periastron	$\omega$	$2.917^{+0.222}_{-0.245}$ (rad)
Stellar mass	$M_*$	$0.703^{+0.068}_{-0.080} M_\odot$
Stellar radius	$R_*$	$0.775^{+0.043}_{-0.040} R_\odot$
Stellar surface gravity	$\log g_*$	$4.51^{+0.06}_{-0.05}$ (CGS)
Stellar density	$\rho_*$	$1.51^{+0.25}_{-0.20} \rho_\odot$
Planet radius	$R_p$	$1.28^{+0.077}_{-0.091} R_J$
Planet mass	$M_p$	$2.96^{+0.22}_{-0.17} M_J$
Planetary surface gravity	$\log g_p$	$3.62 \pm 0.06$ (CGS)
Planet density	$\rho_p$	$1.43^{+0.31}_{-0.29} \rho_J$
Planet temp ( $A = 0$ )	$T_{\text{eq}}$	$1119^{+26}_{-28}$ K
$\chi^2_\nu$ (photometric)	$\chi^2_{\text{phot}}$	4145
Photometric data points	$N_{\text{phot}}$	4151
$\chi^2_\nu$ (spectroscopic)	$\chi^2_{\text{spec}}$	17.2
Spectroscopic data points	$N_{\text{spec}}$	14

One plausible mechanism for maintaining the high eccentricity is secular interaction with an additional planet in the system. Adams & Laughlin (2006) explore the effects of dynamical interactions among planets in extrasolar planetary systems and conclude outer planets can cause the inner planet to move through a range of eccentricities over timescales that are short when compared to the lifetime of the system, but very long when compared to the current observational baseline. However, recently Matsumura et al. (2008) have argued that an unseen companion driving short-Period systems is unlikely. They present an upper limit of  $1 M_{\text{Neptune}}$  for a possible unseen companion in the GJ 436 system and exclude this based on the current radial velocity upper limits of  $\leq 5$  m/s. Matsumura et al. (2008) also present a range of tidal quality  $Q_p$  timescales that could be as large as  $10^9$  years, and argue that this new class of eccentric, short period ESP are simply still in the process of circularizing. WASP-10b has not been extensively studied to rule out a putative outer plane that may be driving its eccentricity. Thus, the  $\approx 6\%$  eccentricity of WASP-10b makes it an attractive target for future transit-timing variation studies, and for longer-term RV monitoring to establish the mass and period of the putative outer planet.

The majority of transiting ESP found have masses be-

low  $1.5M_J$ , although there are a few more massive ESP. HD 17156, and COROT-Exo-2 have similar masses to WASP-10b and although there are two more massive ESP, the nearly  $9 M_J$  HAT P-2 (HD 149026b) (Bakos et al. 2007) and  $7.3 M_J$  WASP-14b (Joshi et al. 2008), this higher mass region has been poorly explored. Additional transiting objects in the mass range are important for completing the current ESP mass-radius relations and constraining their compositions. The current sample of transiting extrasolar giant planets (ESP) reveals a large range of densities. We derive a mean density for WASP-10b of  $\approx 1.89 \text{ g cm}^{-3}$  ( $1.42 \rho_J$ ) and it would lie along the higher density contour in a mass-radius plot (Pollacco et al. 2008; Sozzetti et al. 2007).

One ultimate goal of our transit-search programme is to provide the observational grist that will stimulate and advance refined models for the formation and evolution of the hot and very hot Jupiters (e.g. Burrows et al. 1997; Fortney et al. 2007; Seager et al. 2007). By thus constraining the underlying physics, we will have a richer context for the interpretation of the lower mass planets expected from missions such as COROT and Kepler.

## ACKNOWLEDGMENTS

The SuperWASP Consortium consists of astronomers primarily from the Queen's University Belfast, St Andrews, Keele, Leicester, The Open University, Isaac Newton Group La Palma and Instituto de Astrofísica de Canarias. The SuperWASP Cameras were constructed and operated with funds made available from Consortium Universities and the UK's Science and Technology Facilities Council. SOPHIE observations have been funded by the Optical Infrared Co-ordination Network. The data from the Mercator and NOT telescopes was obtained under the auspices of the International Time of the Canary Islands. We extend our thanks to the staff of the ING and OHP for their continued support of SuperWASP-N and SOPHIE instruments. FPK is grateful to AWE Aldermaston for the award of a William Penney Fellowship.

## REFERENCES

Adams F.C, Laughlin G. 2006, ApJ, 649, 992  
 Anderson D.R. et al. 2008, MNRAS, 387, 4 and ArXiv/0801.1685  
 Bakos G.A. et al., 2007, ApJ, 670, 826  
 Blackwell D.E., Shallis M.J., 1977, MNRAS 180, 177  
 Bouchy F., The Sophie Team, 2006, in Arnold L., Bouchy F., Moutou C., eds, Tenth Anniversary of 51 Peg-b: Status of and prospects for hot Jupiter studies, pp 319 – 325.  
 Burrows A. et al. 1997, ApJ, 491, 856  
 Collier Cameron A., et al., 2007a, MNRAS, 380, 1230  
 Collier Cameron A. et al., 2007b, MNRAS, 375, 951  
 Fortney J.J., Marley M.S., Barnes J.W. 2007, ApJ, 659, 1661  
 Hebb L. et al. 2008, A&A, submitted  
 Hellier C. et al. 2008, ApJ, submitted, & arXiv0805.2600  
 Horne K.D., 2003, Scientific Frontiers of Exoplanet Research, ASP Conf. 294, 361, eds. Deming & Seager (San Francisco)

Jackson, B., Greenberg, R., Barnes, R. 2008, ApJ, 678, 1396  
 Joshi Y.C. et al. 2008, MNRAS, submitted, & arXiv0806.1478  
 Mardling R. 2007, MNRAS, 382, 1768  
 Matsumura S., Takeda G., & Rasio F.A. 2008, ApJ, in press and arXiv:0808.3724  
 Pollacco D. et al., 2006, PASP, 106, 1088  
 Pollacco D. et al., 2008, MNRAS, 385, 1576  
 Queloz D. et al., 2001, A&A, 379, 279  
 Seager S., Kuchner M., Hier-Majumder C.A., Militzer B. 2007, ApJ, 669, 1279  
 Smith A.M.S et al. 2007, MNRAS, 373, 1151  
 Sozzetti A., Torres G., Charbonneau D., Latham D.W., Holman M.J., Winn J.N., Laird J.B., O'Donovan F.T., 2007, preprint (arXiv:astro-ph 0704.2938v1)  
 Stetson, P. 1987, PASP, 99, 191  
 Stempels H.C, Collier Cameron A., Hebb L., Smalley B., Frandsen S., 2007, MNRAS, 379, 773  
 Terndrup D.M. et al. AJ, 119, 1303  
 Torres G., Konacki, M., Sasselov D.D., Jha, S. 2004, ApJ, 614, 979  
 Valenti J.A., Fischer D., 2005 ApJS 159, 141  
 Valenti J.A., Piskunov N., 1996 A&AS, 118, 595  
 West R. et al. 2008, A&A, submitted, & arXiv0809.4597  
 Wilson D. et al. 2008, ApJ, 675, 113

This paper has been typeset from a  $\text{T}_{\text{E}}\text{X}/\text{L}^{\text{A}}\text{T}_{\text{E}}\text{X}$  file prepared by the author.